JOURNAL OF COLLOID AND INTERFACE SCIENCE **194,** 398–407 (1997)
ARTICLE NO. CS975100

Surface Chemical Analysis and Electrokinetic Properties of Spherical Hematite Particles Coated with Yttrium Compounds

R. C. Plaza,* J. D. G. Durán,* A. Quirantes,* M. J. Ariza,† and A. V. Delgado*,[1]

*Departamento de Física Aplicada, Facultad de Ciencias Universidad de Granada, 18071 Granada, Spain †Departamento de Física Aplicada I, Facultad de Ciencias Universidad de Málaga, 23071 Málaga, Spain

Received April 23, 1997; accepted July 24, 1997

We describe in this work the chemical and electrokinetic surface characterization of core–shell particles consisting of a practically spherical hematite nucleus coated by a layer of yttrium basic carbonate or yttrium oxide (obtained after calcination of the carbonate-coated particles, following the method of E. Matijević and B. Aiken (*J. Colloid Interface Sci.* 126, 645 (1988))). The morphological and surface characteristics of the particles were controlled by modifying the initial yttrium nitrate concentration and the growing time. A total of 14 samples of hematite–yttrium basic carbonate composites were obtained, and three of them (obtained by keeping at 90°C solutions containing 6.5×10^{-4} *M* α-Fe_2O_3, 1.8 *M* urea, and 1.1, 3, and 4.9 m*M* $Y(NO_3)_3$, respectively) were then converted into hematite–Y_2O_3 particles. Transmission electron microscopy was used to ascertain the shape and size of the particles. The spherical geometry of the core hematite is found, as a rule, on the core–shell particles; in general, carbonate samples obtained with intermediate initial concentration of $Y(NO_3)_3$ have the maximum coating thickness, whereas increasing that concentration does not lead to thicker coatings. Hence, formation of individual yttrium basic carbonate, together with coated hematite, cannot be completely ruled out under such conditions. Two techniques were employed for the elucidation of the surface composition of the particles, namely EDX and XPS (or ESCA). In particular, XPS data show that the coating of hematite by yttrium carbonate is almost complete in the case of particles obtained with 3 m*M* $Y(NO_3)_3$ concentration and 9-h heating time. The oxide samples obtained after calcination show high contents of yttrium and low iron surface concentration for initial $[Y(NO_3)_3] = 1.1$ m*M* (sample OB9) and 3 m*M*. According to XPS analysis, both types of particles have a quite similar surface composition and structure. For all types of particles but the carbonate-coated ones obtained at the shortest reaction times, the pH_{iep} was found to be above that of pure hematite, approaching that of yttrium basic carbonate or oxide. In particular, among the oxide-coated particles, it is sample OB9 the one that most closely approaches its pH_{iep} to that of Y_2O_3, in good agreement with the surface chemical analysis performed with XPS. © 1997 Academic Press

Key Words: **colloidal hematite coated particles; yttrium oxide and carbonate; core–shell colloidal particles; electrophoresis; surface chemical composition of colloids.**

INTRODUCTION

The preparation and characterization of monodisperse colloidal particles composed of a core particle coated by a shell of a different, controlled composition has received considerable interest, mainly because of the promising technological applications of such systems, but also due to their various physicochemical properties (1–4). From the former point of view, one of the possibilities is of obtaining large amounts (or particles of given size and shape) of the shell compound, with special properties, using only the relatively smaller quantity necessary to coat the cores. The expensive coating material, of which only the surface behavior is of interest, would thus be placed on the (cheaper or easier to obtain) core, imparting the latter most of its surface properties; the stability, rheology, tribology, etc., of the core–shell particles will be primarily dominated by the coating.

In other cases, the properties of both the core and the shell can be of interest. Thus a magnetic core can be useful for controlling the stability or transport properties of the suspensions, whereas the adsorption properties of the shell can be used with advantage with the aim of obtaining composite particles that could be vehicles for the transport and release of, for instance, therapeutical drugs. Magnetic fields can be applied to control the adhesion or removal of the particles and their adsorbed material to and from different substrates (5).

Matijević and his co-workers (1–4) have demonstrated that the synthesis of core–shell particles in controlled conditions (concerning the size and shape of the colloids obtained, as well as the thickness of the coating) is possible for very different systems, including cores like hematite, chromium hydroxide, or titania and coatings like aluminum, zirconium, and yttrium compounds.

In the present work, the method originally described by Aiken and Matijević (4) for the obtention of elongated hematite particles coated with yttrium carbonate or oxide, is applied to the synthesis of core–shell particles with spherical hematite particles covered by yttrium basic carbonate and oxide. Different samples with various coating thicknesses

[1] To whom correspondence should be addressed. E-mail: adelgado@goliat.ugr.es.

0021-9797/97 $25.00

have been obtained, and a thorough analysis of their surface and bulk chemical composition has been carried out, together with a characterization of their electrokinetic properties. A comparison between bare and coated particles will hence be possible on a quantitative basis.

EXPERIMENTAL

A. Materials

The synthesis of the coated particles was carried out in two steps. Spherical hematite core particles were obtained by homogeneous precipitation in aqueous solutions containing 0.018 *M* $FeCl_3$ (Merck, Germany) and 0.001 *M* HCl (Carlo Erba, Italy). One-liter Schott glass flasks were heated for 24 h at 100°C in a convection oven, according to the procedure of Matijević and Scheiner (6). The suspensions obtained were immediately cooled down and then repeatedly centrifuged and redispersed in Milli-Q water, until the conductivity of the supernatant was below 1 μS/cm. The suspensions were further purified by serum replacement until a final conductivity $\leqslant 2$ μS/cm. In order to get rid of the strongly adsorbed chloride ions, a 1 *M* NaOH (Panreac, Spain) solution was added to the suspension and the serum replacement repeated with water. When the conductivity was again as low as before, the cleaning process was considered finished. Hematite suspensions (with a concentration of $\sim$13.9 g/liter) were kept in polyethylene flasks.

Core hematite particles were found to be approximately spherical, quite uniform in size and shape. Their average diameter is 60 $\pm$ 7 nm.

Yttrium basic carbonate was precipitated on hematite following the procedure described in (4): given amounts of bare core particles were mixed with urea (Panreac, Spain) and yttrium nitrate (Merck, Germany) solutions so that the concentrations specified in Table 1 were reached. The suspensions thus obtained were heated in a convection oven at 90°C for the time intervals shown in the table. As observed, 14 different types of α-Fe_2O_3/yttrium basic carbonate were obtained; they will be denoted CA*X*, CB*X*, and CC*X*, when the initial concentration of yttrium nitrate is 1.1, 3, and 4.9 m*M*, respectively. The digits indicate the heating time in hours.

Samples CA9, CB9, and CC9 were chosen to obtain hematite particles coated by yttrium oxide. To do this, the suspensions were first dried at 60°C in a vacuum oven and then calcined at 800°C for 3 h in the presence of air. The oxide-coated particles will be denoted OA9, OB9, and OC9, respectively.

Both carbonate- and oxide-coated particles were cleaned of undesired ions by the method above described for hematite.

TABLE 1

Samples of Hematite–Yttrium Basic Carbonate Composite Particles Obtained by Heating at 90°C Solutions Containing 6.5×10^{-4} *M* α-Fe_2O_3, 1.8 *M* Urea, and the Yttrium Nitrate Concentration Specified

Sample	$[Y(NO_3)_3]$ (m*M*)	Reaction time (h)	D_p (nm)	Specific surface area (m^2/g)
CA2	1.1	2	62 $\pm$ 6	
CA9	1.1	9	170 $\pm$ 30	20.5
CA15	1.1	15	57 $\pm$ 7	
CB2	3	2	100 $\pm$ 30	
CB6	3	6	100 $\pm$ 30	
CB9	3	9	180 $\pm$ 40	26.8
CB12	3	12	75 $\pm$ 15	
CB15	3	15	110 $\pm$ 15	
CC2	4.9	2	150 $\pm$ 40	
CC9	4.9	9	125 $\pm$ 40	13.2
CC15	4.9	15	130 $\pm$ 30	

Note. Average particle diameters (TEM; $\pm$SD) and specific surface areas of representative samples are also included.

B. Methods

The morphological characteristics of the particles were analyzed by transmission electron microscopy. Indirect information about the size of the colloidal particles and their porosity was also obtained by surface area measurements using a Quantasorb Jr. (Quantachrome, USA), based on the BET multipoint method, with nitrogen as adsorbent.

Surface chemical composition was elucidated by means of two techniques: EDX (energy dispersion of X-rays, Carl Zeiss DSM 950 SEM, Germany) and XPS (X-ray photoelectron spectroscopy or ESCA, Perkin-Elmer, USA). The former yields information about the atomic composition in a region comparable to the diameter of the electron beam (0.1–10 μm) and $\leqslant$500 Å in depth. The experimental error of the method can be estimated as $\pm$0.5% atomic content (7). XPS provides more precise information on the surface composition (it probes only the first few outermost atomic layers) of a larger area (several mm^2), with a comparable sensitivity of $\pm$0.5% (8).

The electrokinetic properties of the particles were analyzed as a function of pH, for different NaCl concentrations, by measuring their electrophoretic mobility, μ_e, at 25.0 $\pm$ 0.5°C in a Malvern Zetasizer 2c (Malvern Instruments, England). The relative error in μ_e determinations is about 5%.

RESULTS AND DISCUSSION

Particle Morphology

Figure 1 shows TEM pictures of some of the particles obtained (yttrium basic carbonate coated hematite, samples

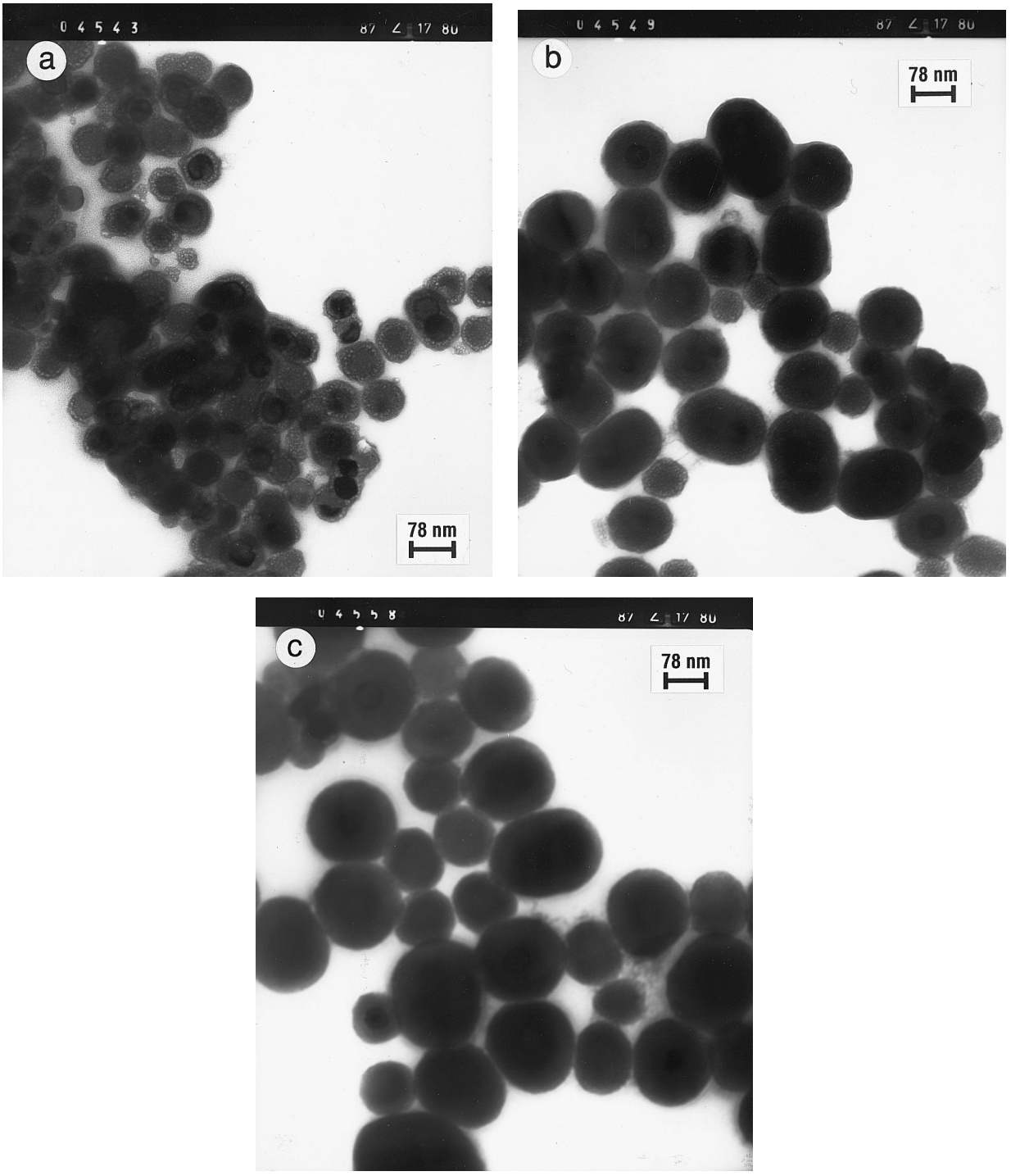

FIG. 1. TEM pictures of hematite particles coated with yttrium basic carbonate. (a) Sample CA9 of Table 1, (b) sample CB9, (c) sample CC9.

CA9, CB9, CC9). As observed, coated particles are reasonably spherical in shape, although they are more polydisperse than the original core particles. The polydispersity is not, however, the same for all kinds of particles; from the comparison between the three pictures, it can be concluded that sample CC9 appears to be the most polydisperse, and also the one with the thickest coating around individual particles. The hematite cores are visible in most cases. Note also that the possibility that two particles share the same shell cannot be discarded, mainly in the case of samples CB9 and CC9.

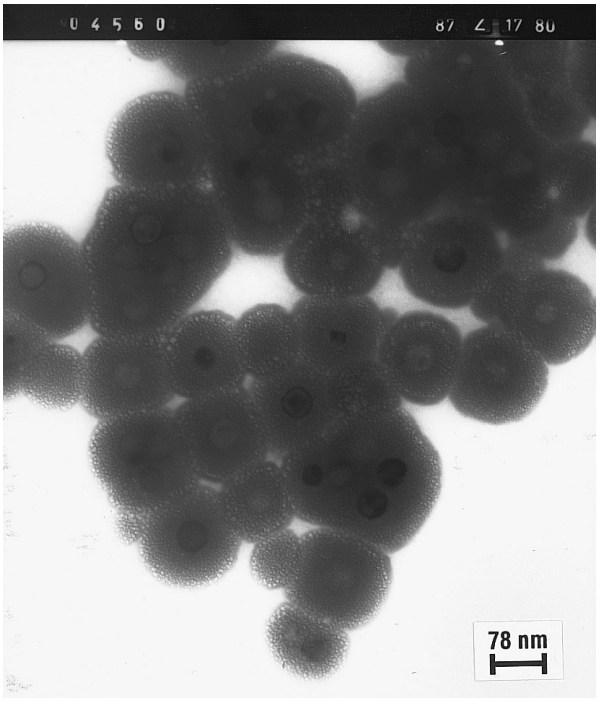

FIG. 2. TEM micrograph of sample CC15.

The average particle diameters obtained from TEM micrographs similar to those shown in Fig. 1 are included in Table 1. Let us analyze the effect of the synthesis conditions on the obtained particles. Considering the initial yttrium nitrate concentration (compare samples CA, CB, and CC for equal reaction times), data in Table I show that, in general, samples of CB with intermediate concentration have the maximum coating thickness. It is noticeable that increasing $[Y(NO_3)_3]$ does not systematically lead to thicker coatings; hence, the possibility that yttrium basic carbonate particles are formed together with coated hematite cannot be ruled out in the case of CC samples.

Concerning the relationship between reaction time and particle diameter—for given yttrium nitrate concentration—Table 1 shows that 9 h is the optimum time for obtaining a high degree of coating. Shorter precipitation times seem to be insufficient for obtaining enough coverage of hematite by yttrium carbonate, whereas if the reaction proceeds above 9 hours, it is possible that the coating detaches from the particles and individual yttrium carbonate particles are formed. This seems to be confirmed by the observation that particles obtained at long reaction times are more polydisperse (Table 1) and less homogeneous in shape, with a significant fraction of particles formed by two or more cores with a common shell (Fig. 2 is an example).

Specific surface area data of the samples obtained after the optimum reaction time, 9 h (CA9, CB9, and CC9), are included in Table 1 (the value for core particles is 20.9 m^2/g). As observed, the surface area of CA9 is comparable to that of the hematite core; this is an indirect confirmation of the relatively small thickness of the coating in sample CA. The moderate increase in specific surface area from CA9 to CB9 can be explained by the apparently porous structure of the coating (see Fig. 2, for instance), which overcompensates for the size increase found between those two samples. Concerning sample CC9, the surface area is clearly lower and the effect of size increase predominates in this case over the opposed effect of the yttrium carbonate shell.

After calcination, particles like those shown in Fig. 3 were obtained. Comparison between these pictures and those in Fig. 1 visually demonstrates the structural changes that have taken place. The coating is much more compact and opaque to electrons in the case of Y_2O_3–hematite composites, probably as a consequence of the crystallinity of ytrium oxide–demonstrated by XRD data not shown here—as opposed to the amorphous nature of yttrium carbonate. By image analysis of the TEM pictures (including more than 200 particles in all cases), the particle diameters were estimated to be 130 ± 20, 150 ± 20, and 110 ± 20 nm for samples OA9, OB9, and OC9, respectively. Comparison of these figures with data corresponding to CA9, CB9, and CC9 demonstrates the shrinkage that, as mentioned above, occurs in the coating layer upon calcination.

The Transformation from Yttrium Basic Carbonate to Yttrium Oxide (4)

As already done by other authors, the physical changes involved in the transformation of the coating from carbonate to oxide were followed by thermogravimetric analysis (TGA). A Shimadzu TGA-50H was used at a heating rate of 20°C/min in air, to perform the analysis on samples CA9, CB9, and CC9. The scans obtained are shown in Fig. 4. Since the thermal treatment (maximum temperature: 1000°C) does not induce any physical transformation in the hematite core (4, 9), all events shown in Fig. 4 must be associated to the $Y(OH)CO_3$ coating.

Sordelet and Akinc (10) demonstrated that at about 180°C the weight loss is associated to water loss and decomposition of the hydroxycarbonate to oxicarbonate, according to the scheme

$$2Y(OH)CO_3 \rightarrow (180°C) \rightarrow Y_2O_2CO_3 + H_2O + CO_2,$$

and another important transformation occurs when the temperature reaches 610–700°C, when the vaporization is complete, and the amorphous oxicarbonate transforms into crystalline cubic yttrium oxide:

$$Y_2O_2CO_3 \rightarrow (610–700°C) \rightarrow Y_2O_3 + CO_2.$$

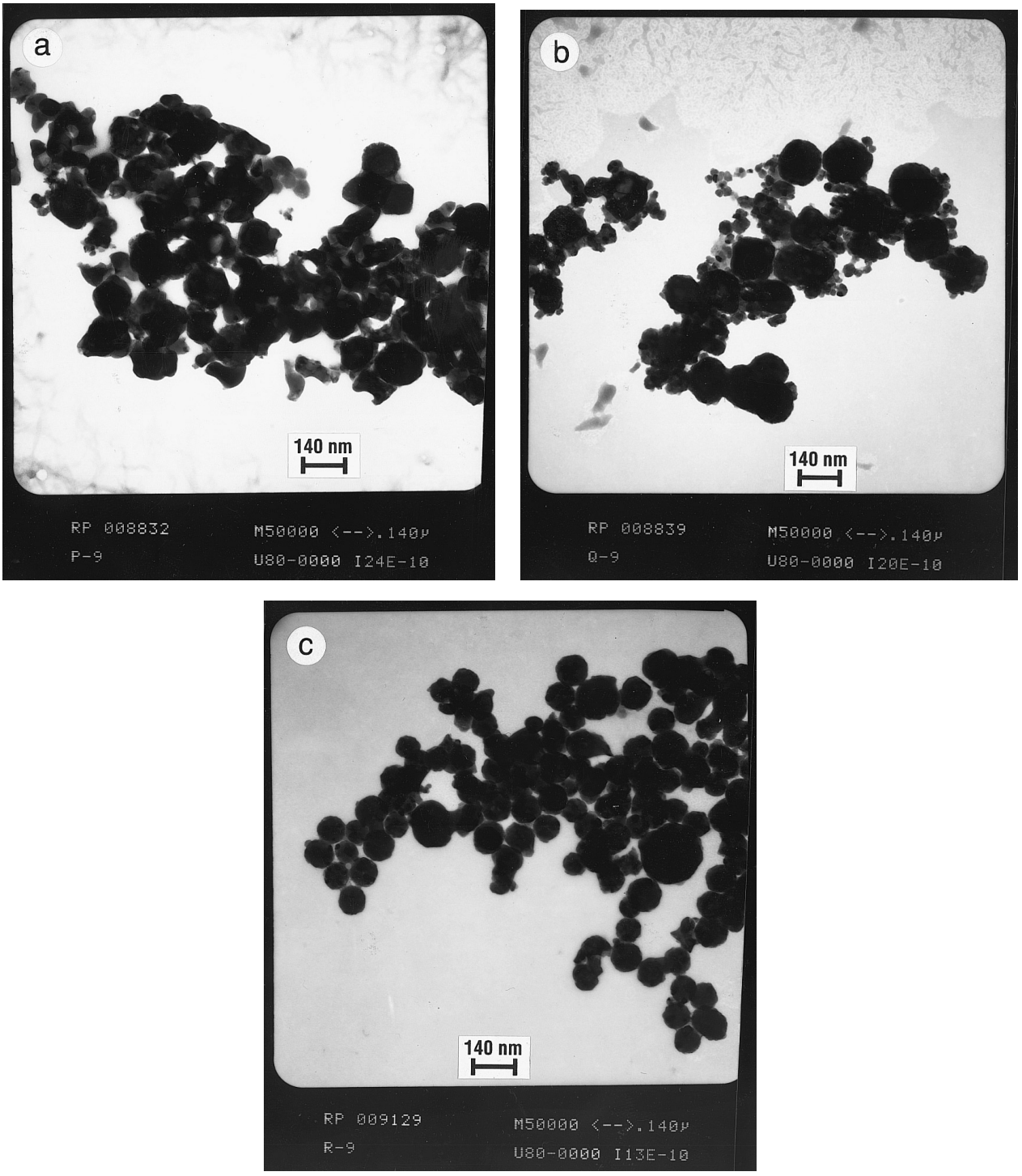

FIG. 3. Transmission electron micrographs of hematite particles coated by yttrium oxide. (a) Sample OA9, (b) sample OB9, (c) sample OC9.

Similar conclusions were reached by Aiken and Matijević (4) and Kawahashi and Matijević (11).

All our samples show a gradual, moderate weight loss below ~200°C and above ~700°C, the most important changes taking place between these two temperatures. A characteristic peak is observed in sample CC9 at ~660°C, whereas the other samples show peaks at ~580 and ~750°C (CA9) and ~530 and ~650°C (CB9). Such events must correspond to the transformation from carbonate to oxide, and the subsequent CO_2 loss. This was

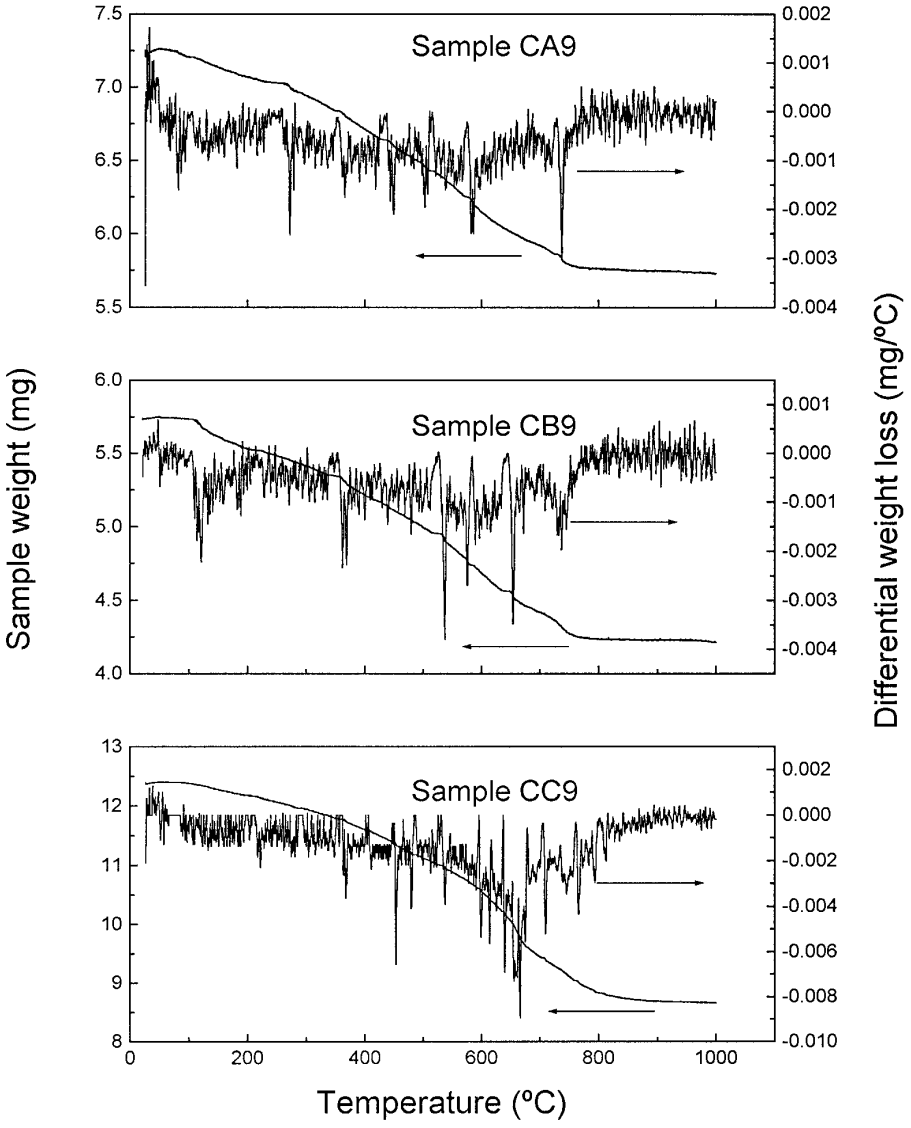

FIG. 4. TGA results on samples CA9, CB9, and CC9.

confirmed by IR analysis of the gases produced during calcination.

As a rule, the loss rate increases in the order CA9 < CB9 < CC9, that is, in the order of increasing initial $Y(NO_3)_3$ concentration. This suggests that the yttrium content of the samples increases in the same order. Since, according to TEM data, the coating of sample CC9 is not always thicker than that of samples CA9 or CB9, TGA results seem to confirm the formation of $Y(OH)CO_3$ not only on hematite, but also free in solution, when the initial yttrium concentration is high (samples CC).

Surface Chemical Analysis

EDX microanalysis of the carbonate-coated particles did not allow the reaching of any precise conclusion about their chemical composition. The only clear result is the presence of yttrium and iron and not any other metallic element. On the contrary, the EDX spectra of the calcined samples (OA9, OB9, and OC9) allowed more quantitative conclusions. Table 2 shows the percentage content of oxygen, yttrium, and iron in the samples; because of the small size of the probing electron beam, data were taken in three different positions of each specimen. These individual data, together with their average values, have been included in the table.

As observed, the oxygen content is very similar in the three samples, although the relative amount of this element is slightly larger in sample OA9; more significant are the differences in yttrium and iron. The former changes in the order

TABLE 2
EDX Spectra of Oxide-Coated Hematite Particles OA9, OB9, and OC9

Sample	X-ray line	Percentage content[a]	Average (±SD)
OA9	O K_α (0.46–0.56 keV)	13.6/8.2/8.9	10.3 ± 2.4
	Y L_α (1.84–1.98 keV)	31.7/38.3/35.1	35 ± 3
	Y L_β (1.92–2.04 keV)	8.3/9.3/9.9	9.2 ± 0.7
	Fe K_α (6.30–6.48 keV)	41.9/39.0/40.7	40.5 ± 1.2
	Fe K_β (6.94–7.14 keV)	4.6/5.1/5.4	5.0 ± 0.3
OB9	O K_α	8.7/5.5/6.8	7.0 ± 1.3
	Y L_α	62.9/69.8/66.0	66 ± 3
	Y L_β	19.0/16.5/14.0	16.5 ± 2.1
	Fe K_α	9.3/7.5/12.2	9.7 ± 1.9
	Fe K_β	0.05/0.6/1.0	0.6 ± 0.4
OC9	O K_α	4.7/5.7/6.0	5.5 ± 0.5
	Y L_α	70.5/69.8/71.1	70.5 ± 0.5
	Y L_β	14.4/11.7/14.5	13.5 ± 1.3
	Fe K_α	9.3/11.5/7.5	9.4 ± 1.7
	Fe K_β	1.0/1.3/0.9	1.1 ± 0.2

Note. Elements analyzed: oxygen, yttrium, and iron.
[a] Data corresponding to three different surface regions probed.

$$\text{OA9} < \text{OB9} \simeq \text{OC9},$$

whereas the estimated amount of iron follows the sequence

$$\text{OA9} > \text{OB9} \simeq \text{OC9}.$$

It is worthwhile to point out that about 40% of sample OA9 is iron, this figure dropping to ~9% in OB9 and OC9. Given the depth probed by incident electrons (~500 Å, as mentioned above), it is clear that OA9 has a thinner (or less compact) coating than the other two samples. The comparison between yttrium concentrations (~40% in OA9 and ~80% in OB9 or OC9) also points to this conclusion. Furthermore, the high Y content in OB9 and OC9 demonstrates that hematite cores are well coated by Y_2O_3, although data mentioned above do not rule out the possibility of pure Y_2O_3 particles in the system. This analysis must be, in any case, reconsidered in the light of XPS data (to be discussed below), since XPS provides information only on the actual surface composition.

From XPS spectra of one of the carbonate samples (CC9) and the three oxide-coated particles (OA9, OB9, OC9), the peak features detailed in Table 3 were obtained. In this table, the binding energies are corrected for the shift due to sample charging; values of this shift (−3.25, −4.25, −5.125, and −5.0 eV, respectively, for the four samples) were obtained by comparing the theoretical (12) and experimental position of the peaks.

From these data, it is clear that the coating of the hematite core by $Y(OH)CO_3$ is practically complete in sample CC9, since only 0.12% surface iron is detected. The carbon amount associated to carbonate is large compared to that found in the oxide samples, and the peak is very well defined. Hence, athough the carbonate content in samples OA9, OB9, and OC9 can be ascribed to surface contamination during sample manipulation, in the case of CC9, the carbonate coating is clearly manifested.

Considering now the chemical composition of oxide samples, the following features must be mentioned:

(i) The amount of surface C is comparable in the three oxide samples (12–14%), and, as mentioned above, its low values are ascribed to contamination of the surface by carbonates or carbon oxides.

(ii) The surface concentration of oxygen is also similar in the three samples (confirming results of our EDX analysis).

(iii) The amounts of yttrium and iron change according to the sequence

$$\text{Fe (OA9)} > \text{Fe (OB9)} \approx \text{Fe (OC9)}$$
$$\text{Y (OA9)} < \text{Y (OB9)} \approx \text{Y (OC9)},$$

also in good agreement with EDX data in Table 2. Hence, the conclusion can be reached that the coating of sample OA9 is not complete, whereas samples OB9 and OC9 have very similar surface structure, with thick coatings, and, possibly, formation of Y_2O_3 particles.

Electrokinetic Characterization

Electrokinetic measurements can be an excellent probe (indirect, however) of the surface characteristics of a ma-

TABLE 3
XPS Data for Samples CCP (Hematite/$Y(OH)CO_3$), OA9, OB9, and OC9 (Hematite/Y_2O_3)

Sample	Peak	Binding energy (eV)		Peak area[a] (a.u.)	Atomic percent
		Oxide	Carbonate		
CC9	C 1s	285	290.1	29,357	35.2
	O 1s	—	531.7	101,452	48.6
	Fe $2p^{3/2}$	710.4	—	1,000	0.12
	Y $3d^{5/2}$	—	153.6	82,658	16.0
OA9	C 1s	285	290.6	7,858	14.3
	O 1s	529.3	531.4	71,382	52.0
	Fe $2p^{3/2}$	710.4	—	52,630	10.0
	Y $3d^{5/2}$	157.0	—	80,274	23.6
OB9	C 1s	285	290.1	6,500	12.4
	O 1s	529.1	531.6	68,444	52.3
	Fe $2p^{3/2}$	710.1	—	9,414	1.9
	Y $3d^{5/2}$	156.7	—	108,376	33.4
OC9	C 1s	285	290.2	6,093	12.7
	O 1s	529.2	531.5	63,240	52.9
	Fe $2p^{3/2}$	710.4	—	14,869	3.2
	Y $3d^{5/2}$	156.9	—	91,991	31.1

[a] These areas must be corrected for the sensitivity factors provided by the manufacturer (12).

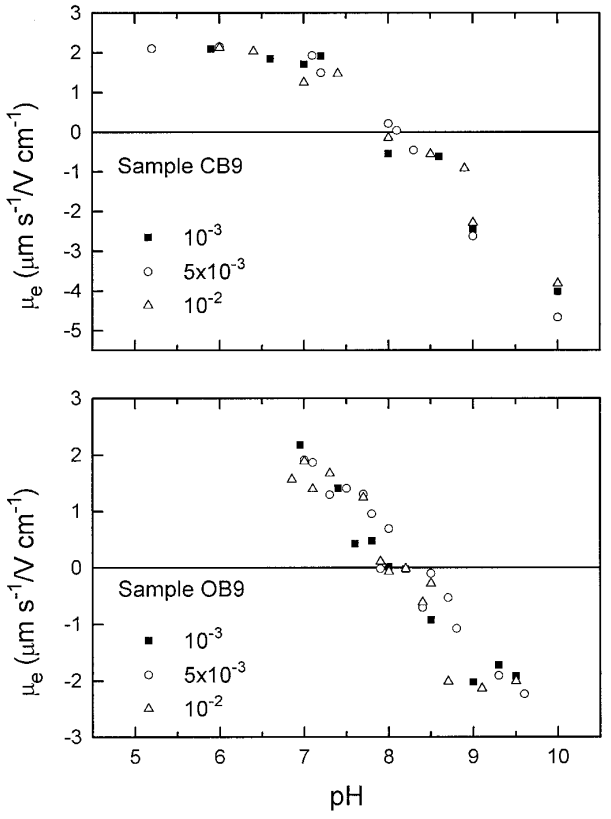

FIG. 5. Electrophoretic mobility of coated samples CB9 ($Y(OH)CO_3$) and OB9 (Y_2O_3), as a function of pH, for different NaCl molar concentrations.

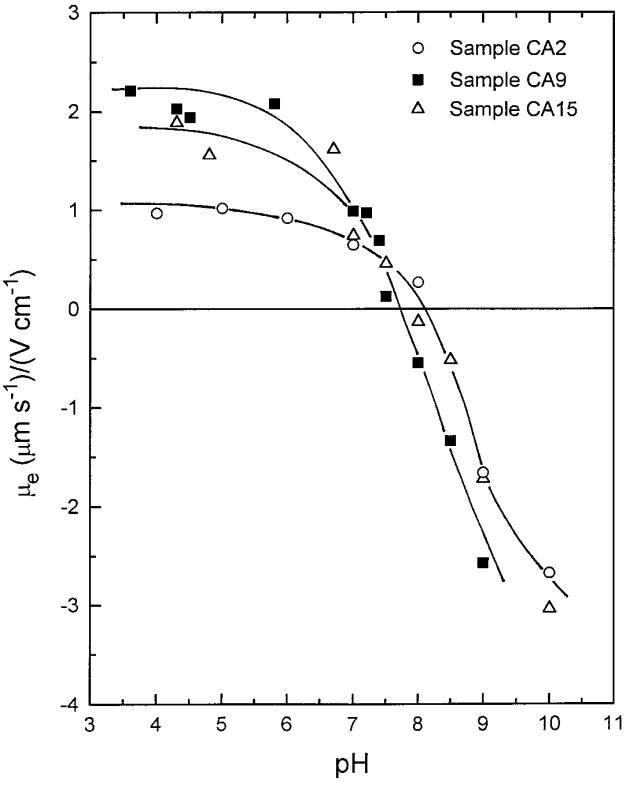

FIG. 6. Electrophoretic mobility of CA samples as a function of pH, in 5×10^{-3} *M* NaCl solution.

terial. In particular, the value of the isoelectric point (pH_{iep}, or pH of zero zeta potential) of the solid, for different ionic compositions of the dispersion medium, has been considered as a ''fingerprint'' of the material under study (13). Hence, this kind of test was also carried out with suspensions of the coated hematite particles described in this work. Our goal was to analyze the changes in iep for the different synthesis conditions.

Previous work by other authors (11, 14, 15) shows that, with slight fluctuations from one article to another, the pH_{iep} of yttrium carbonate or oxide is about 1–1.5 pH units above that of pure hematite particles. Our measurements of electrophoretic mobility of pure hematite in the presence of different NaCl concentrations yielded a pH_{iep} of 7.4–7.6, in good agreement with previous determinations.

A similar type of dependence between electrophoretic mobility, pH, and sodium chloride concentration was found in the case of $Y(OH)CO_3$- and Y_2O_3-coated particles. Figure 5 is an example, corresponding to μ_e data of samples CB9 and OB9. To avoid unncessary crowding of data, only the plots corresponding to an intermediate ionic strength (5×10^{-3} *M* NaCl) will be presented for all samples. Figure 6 corresponds to CA samples, Fig. 7 to

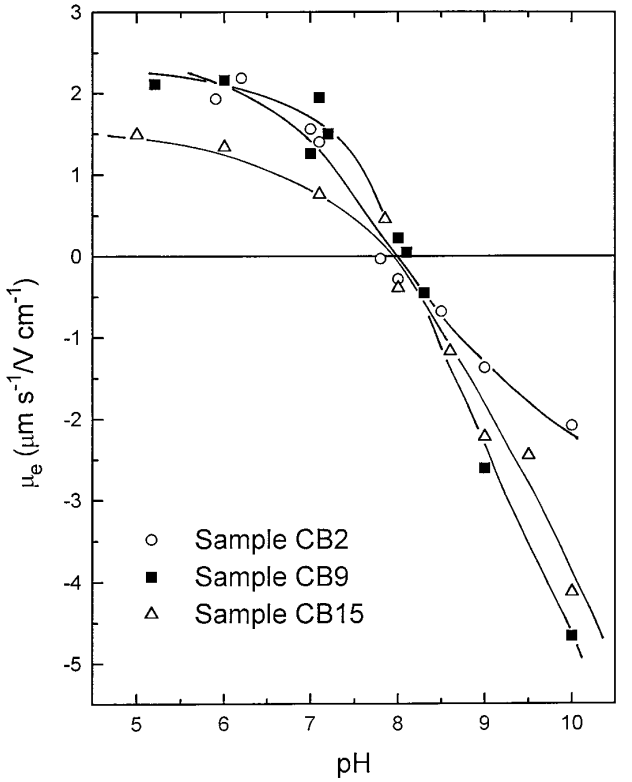

FIG. 7. Same as Fig. 6, for samples CB.

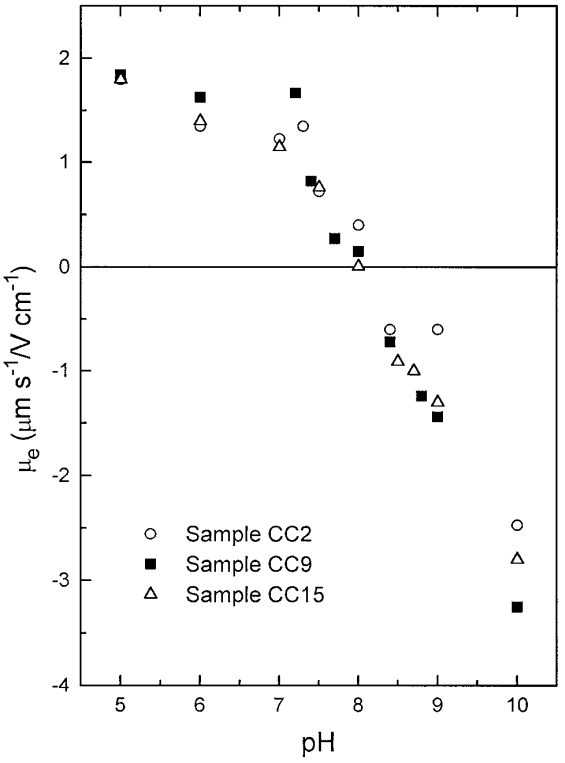

FIG. 8. Same as Fig. 6, for samples CC.

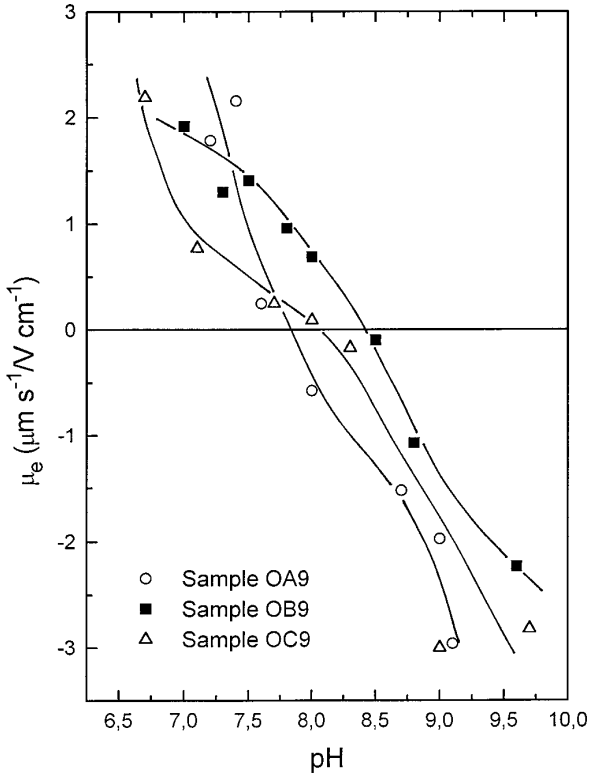

FIG. 9. Electrophoretic mobility of Y_2O_3-coated hematite (samples OA9, OB9, OC9) as a function of pH. Ionic strength: 5×10^{-3} *M* NaCl.

TABLE 4
Values of pH_{iep} of Carbonate and Oxide Coated Particles

Sample	pH_{iep}	Fig. no.
CA2	8.0	6
CA9	7.7	6
CA15	8.0	6
CB2	7.7	7
CB6	8.1	—
CB9	8.1	5, 7
CB12	7.9	—
CB15	7.9	7
CC2	8.3	8
CC9	8.0	8
CC15	8.0	8
OA9	7.8	9
OB9	8.5	5, 9
OC9	8.1	9

Note. Ionic strength: 5×10^{-3} *M* NaCl. Figure numbers where μ_e data can be found are also included.

CB samples, and Fig. 8 to CC samples. The oxide-coated particles showed the electrophoretic mobilities plotted in Fig. 9. From these figures (for brevity, mobility data for samples CB6 and CB15 are not shown), a list of values of pH_{iep} for all samples was obtained, as shown in Table 4. As observed, the pH_{iep} of all the samples is above that of pure hematite, approaching the values of yttrium carbonate and oxide. This shows that the electrical surface properties progressively approach those of the yttrium compounds, as the coating is more efficient. The values shown in Table 4 are, however, systematically lower than those found by, for instance, Sprycha *et al.* (14). However, our own (unpublished) data on the electrophoretic mobility of yttrium carbonate and oxide prepared as described in this paper, but in the absence of hematite, yielded a pH_{iep} of 8.0 ± 0.1 and 8.6 ± 0.1, respectively. Among the carbonate samples in Table 4, it is CB9 and CC9 that more closely approach the electrokinetic behavior of pure yttrium basic carbonate; as to the oxide-coated samples, OB9 is the one that seems to be most efficiently covered by Y_2O_3, since its isoelectric point is very similar to those found by our determinations on yttrium oxide. This is in perfect agreement with our chemical analysis by XPS (see above).

ACKNOWLEDGMENT

Financial support by DGICYT, Spain (Project No. PB94-0812-C02) is gratefully acknowledged.

REFERENCES

1. Gherardi, P., and Matijević, E., *J. Colloid Interface Sci.* **109,** 57 (1986).
2. Kratohvil, S., and Matijević, E., *Adv. Ceram. Mater.* **118,** 506 (1987).

3. Garg, A., and Matijević, E., *Langmuir* **4,** 38 (1988).
4. Aiken, B., and Matijević, E., *J. Colloid Interface Sci.* **126,** 645 (1988).
5. Craig, D. Q. M., *in* ''Technological Applications of Dispersions'' (R. B. McKay, Ed.), p. 457. Dekker, New York, 1994.
6. Matijević, E., and Scheiner, P., *J. Colloid Interface Sci.* **63,** 509 (1978).
7. Grundy, P. J., and Jones, G. A., ''Electron Microscopy in the Study of Materials.'' Edward Arnold, London, 1976.
8. Watts, J. F., *Vacuum* **45,** 653 (1994).
9. Mackenzie, R. C., and Berggren, G., *in* ''Differential Thermal Analysis'' (R. C. Mackenzie, Ed.), pp. 272–299. Academic Press, New York, 1970.
10. Sordelet, D., and Akinc, M., *J. Colloid Interface Sci.* **122,** 47 (1988).
11. Kawahashi, N., and Matijević, E., *J. Colloid Interface Sci.* **143,** 103 (1991).
12. Perkin-Elmer Corporation Physical Electronics Division, XPS User Manual. Minnesota, 1992.
13. Marlow, B. J., and Rowell, R. L., *Langmuir* **7,** 2970 (1991)
14. Sprycha, R., Jablonsky, J., and Matijević, E., *J. Colloid Interface Sci.* **149,** 561 (1992).
15. Matijević, E., Kuo, R. J., and Holuy, H., *J. Colloid Interface Sci.* **80,** 94 (1981).